



2950 Niles Road, St. Joseph, MI 49085-9659, USA  
269.429.0300 fax 269.429.3852 hq@asabe.org www.asabe.org

*An ASABE Meeting Presentation*

*Paper Number: 084761*

## **Open and Closed Loop System Characteristics of a Tractor and an Implement Dynamic Model**

**Manoj Karkee**

Agricultural and Biosystems Engineering Department, Iowa State University,  
karkee@iastate.edu.

**Brian L. Steward**

Agricultural and Biosystems Engineering Department, Iowa State University,  
bsteward@iastate.edu.

**Written for presentation at the  
2008 ASABE Annual International Meeting  
Sponsored by ASABE  
Rhode Island Convention Center  
Providence, Rhode Island  
June 29 – July 2, 2008**

**Abstract.** *Accurate guidance of towed implements is important for performing agricultural field operations and for gaining the ultimate benefit from an agricultural automatic guidance system. The study of open and closed loop system responses can be helpful in the design of practical guidance controllers. A dynamic model of a tractor and a towed implement system was developed. Open loop analysis of the kinematic and dynamic models revealed that the dynamic model was essential for capturing the higher order dynamics of the tractor and implement system at higher operating velocities. In addition, a higher fidelity dynamic model was also developed by incorporating steering dynamics and tire relaxation length dynamics. Closed loop system characteristics were studied by using a linear quadratic regulator (LQR) controller. The tractor position and heading and implement heading states along with respective rate states were fed back to close the loop. The higher fidelity closed loop system used a practical range of steering angles and rates to keep the response within nominal off-road vehicle guidance controller design specifications in the forward velocity range of 0.5 m/s to 10 m/s (1.8 km/h to 36 km/h). These simulation studies provided understanding about the characteristics of the tractor and towed implement system and showed promise in assisting in the development of automatic guidance controllers.*

**Keywords.** dynamic vehicle model, implement guidance, automatic guidance, LQR design, relaxation length

# 1. Introduction

Automatic guidance of agricultural equipment has been an active research area for several decades. The study of relative position based guidance systems was started in the 1970's and 1980's (Julian, 1971; Gerris and Surbrook, 1984; Smith et al., 1985), and continued into the 1990's and new millennium (Chi et al., 1990; Benson et al., 2001). In the mid and late 90's, excited by the successful application of Global Positioning System (GPS) in navigating airplanes and marine vehicles, researchers started applying high accuracy GPS signals to automatically guide agricultural equipment (O'Connor et al., 1996; O'Connor, 1997; Bell, 1997; Stombaugh et al., 1999). In contrast to vision-based or other relative position sensors, GPS provided absolute position and bearing measurements of agricultural vehicles. Due to its global availability and relatively low cost, GPS technology was key in bringing agricultural automation technology up to a new level.

In the past decade, several researchers developed automatic steering controllers to guide agricultural vehicles to straight and curved paths. Stombaugh et al. (1999) developed a GPS-based navigation controller using a double integrator vehicle model. The steering controller was based on a second order derivative transfer function. The controller was stable for velocities less than 6.8 m/s. Bell (2000) developed a linear quadratic regulator (LQR) steering controller based on a kinematic tractor model. Bevely et al. (2002) developed a system identification (ID) based tractor model and compared the performance of the automatic steering controllers designed based on the kinematic, dynamic and system ID-based models.

These automatic guidance controllers used position and/or heading feedback from only tractor mounted sensor(s). To make the agricultural automation widely acceptable, the capabilities of the automatic guidance systems must be extended to implements as well (Bevely, 2001). In the end, it is the implement which often performs the field operation and as such navigating the implement is equally or even more important than guiding the tractor (Karkee et al., 2007).

Some researchers have developed guidance controllers for tractor-and-implement systems. O'Connor et al. (1996) and O'Connor (1997) developed an automatic steering controller based on a kinematic tractor-and-implement model. They designed a hybrid controller to provide a fast response to large errors. A coarse steering command was generated by a non-linear control law. When the errors were reduced to certain threshold level, an LQR controller took over. Bell (1997) developed a kinematic model of a tractor-and-implement system and designed an automatic tracking LQR controller. He demonstrated that implement control is possible, but is more problematic due to the need of steering angles larger than the practical limit and difficulties in estimating position and attitude of the implement without a sensor on the implement. Takigawa et al. (1998) developed a trajectory control method for an agricultural vehicle and a mounted implement system. The feedback controller was designed based on a kinematic vehicle model. Also based on a kinematic model, Karkee et al. (2007) developed an integrated position and heading feedback controller for a tractor-and-implement system. Simulation results showed that the tractor-and-implement steering controller can meet the nominal design specifications of 16 s settling time and 10% maximum overshoot.

One common element in all tractor-and-implement tracking controller design studies was that they used a kinematic tractor-and-implement model. Because the model neglects important dynamics at higher velocities, a kinematic model based guidance controller goes unstable at higher velocities (Bevely et al., 2002). Development of tractor and implement dynamic models and the study of the open and closed loop system characteristics is essential to better understanding the system and developing a robust guidance controller. Another limitation of these tractor and implement guidance controllers was that only the implement position and

heading were feedback to the controllers and the tractor position and heading were neglected. A simultaneous tractor position and heading, and implement position and heading feedback guidance system is essential to get the real benefit from the automatic steering controller.

The objectives of this work were to:

- Develop a dynamic model of a tractor and towed implement system
- Study the open and closed loop characteristics of the tractor and implement system and evaluate the response of the closed loop system

## 2. Dynamic Bicycle Model of a Tractor and Towed Implement System

A dynamic model was developed for a tractor-and-wheeled-towed-implement system (called tractor-and-implement system in the text to follow, Fig. 1). This model, took a “bicycle” approach meaning that the lateral forces in the left and right wheels were assumed to be equal and summed together, and front wheel steering was used. The system was constrained to only allow yawing and lateral motion with a constant forward tractor velocity. The model thus included lateral velocity and yaw rate states for the tractor and a yaw rate state for the implement, which were driven by the lateral tire forces generated through tire side slip. The tractor and the implement rigid bodies were linked by a revolute joint at the hitch point (Feng et al., 2005). The tractor and implement velocities were coupled to each other using the constraint caused by the joint. Common vehicle dynamics symbols were used to describe the dynamics of the tractor-and-implement system (for notation, see the list of the variables).

For a constant forward velocity, the yaw plane lateral motion is given by (Greenwood, 1969),

$$m^t(\dot{v}_c^t + u_c^t \gamma^t) = F_{x,f}^t \sin \delta + F_{y,f}^t \cos \delta + F_{y,r}^t + F_{y,p}^t \quad (1)$$

Similarly, yaw motion is given by,

$$I_{z,c}^t \dot{\gamma}^t = a(F_{x,f}^t \sin \delta + F_{y,f}^t \cos \delta) - bF_{y,r}^t - cF_{y,p}^t \quad (2)$$

Assuming small angle  $\delta$  and further linearizing the equations,

$$m^t(\dot{v}_c^t + u_c^t \gamma^t) = F_{y,f}^t + F_{y,r}^t + F_{y,p}^t \quad (3)$$

$$I_{z,c}^t \dot{\gamma}^t = aF_{y,f}^t - bF_{y,r}^t - cF_{y,p}^t \quad (4)$$

The velocity of the tractor at the hitch point, p, is given by (Greenwood, 1965),

$$u_p^t = u_c^t \quad (5) \quad v_p^t = v_c^t - c\gamma^t \quad (6)$$

Resolving in the implement coordinates,

$$u_p^i = u_c^t \cos \lambda - (v_c^t - c\gamma^t) \sin \lambda \quad (7) \quad v_p^i = u_c^t \sin \lambda + (v_c^t - c\gamma^t) \cos \lambda \quad (8)$$

Translating the hitch point velocities to the implement CG,

$$u_c^i = u_p^i = u_c^t \cos \lambda - (v_c^t - c\gamma^t) \sin \lambda \quad (9)$$

$$v_c^i = v_p^i - d\gamma^i = u_c^t \sin \lambda + (v_c^t - c\gamma^t) \cos \lambda - d\gamma^i \quad (10)$$

Taking derivatives, the lateral acceleration is,

$$\dot{v}_c^i = \dot{u}_c^t \sin \lambda + u_c^t \cos \lambda \dot{\lambda} + (\dot{v}_c^t - c\dot{\gamma}^t) \cos \lambda - (v_c^t - c\gamma^t) \sin \lambda \dot{\lambda} - d\dot{\gamma}^i \quad (11)$$

Assuming a small angle  $\lambda$  and further linearizing the system,

$$u_c^i = u_c^t \quad (12) \quad v_c^i = (v_c^t - c\gamma^t) - d\gamma^i \quad (13)$$

$$\dot{v}_c^i = u_c^t \dot{\lambda} + (\dot{v}_c^t - c\dot{\gamma}^t) - d\dot{\gamma}^i \quad (14)$$

Now, the implement lateral motion is given by,

$$m^i(\dot{v}_c^i + u_c^i \gamma^i) = F_{y,p}^i + F_{y,r}^i \quad (15)$$

Substituting eq. 14 to eq. 15 and solving for  $F_{y,p}^i$ ,



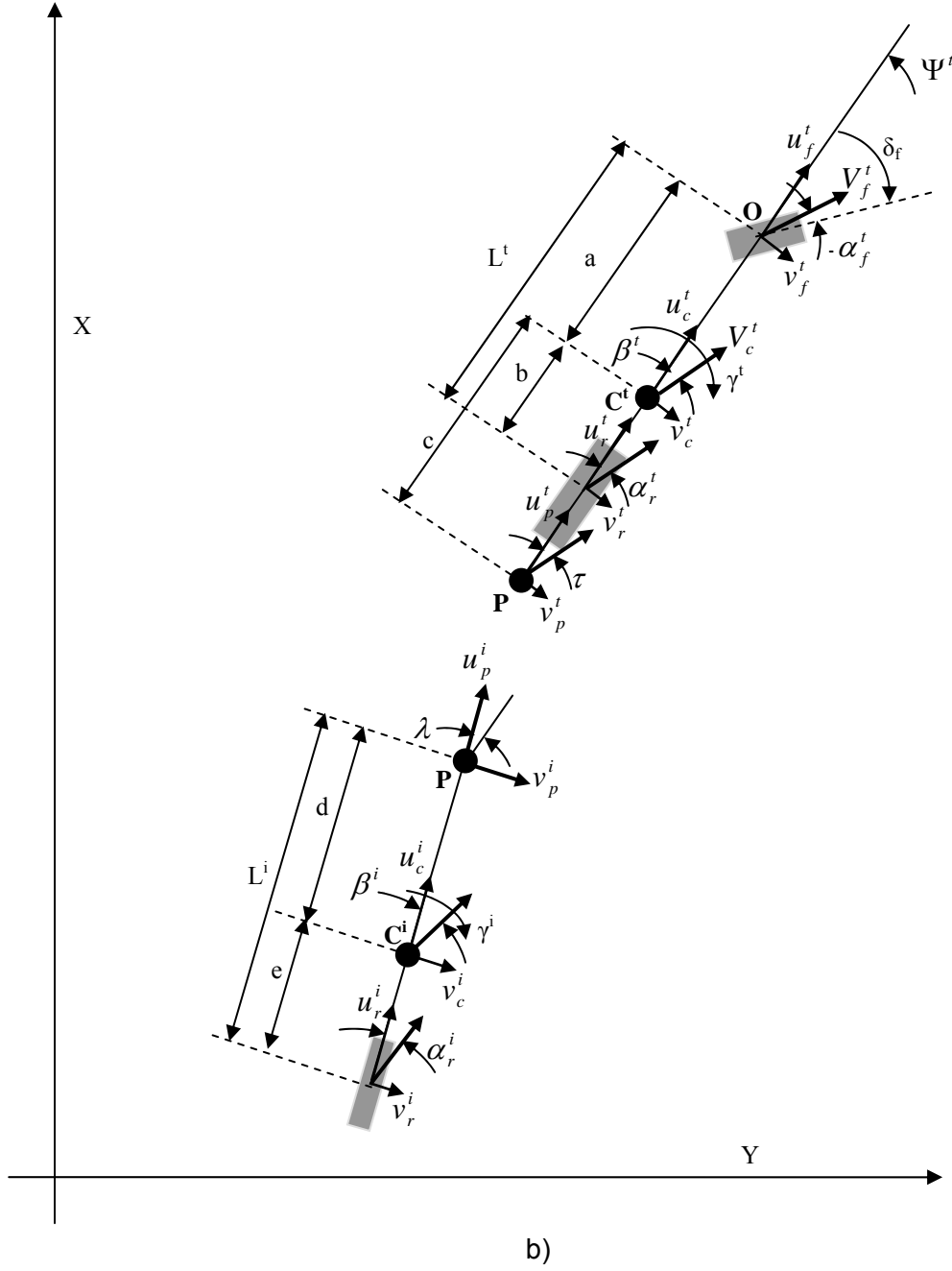


Fig. 1: Dynamic bicycle model of a tractor-and-towed-implement system; a) forces on the system, and b) velocities at different locations of the system.

For a small angle  $\lambda$ ,  $F_{y,p}^t = F_{y,p}^i$ . From eqs. 3 and 4,

$$m^t(\dot{v}_c^t + u_c^t \gamma^t) = F_{y,f}^t + F_{y,r}^t - \{m^i(u_c^t \dot{\lambda} + (\dot{v}_c^t - c \dot{\gamma}^t) - d \dot{\gamma}^i + u_c^t \gamma^i) - F_{y,r}^i\} \quad (17)$$

$$I_{z,c}^t \dot{\gamma}^t = a F_{y,f}^t - b F_{y,r}^t + c \{m^i(u_c^t \dot{\lambda} + (\dot{v}_c^t - c \dot{\gamma}^t) - d \dot{\gamma}^i + u_c^t \gamma^i) - F_{y,r}^i\} \quad (18)$$

The yaw dynamics of the implement are given by,

$$I_{z,c}^i \dot{\gamma}^i = m^i d \{u_c^t \dot{\lambda} + (\dot{v}_c^t - c \dot{\gamma}^t) - d \dot{\gamma}^i + u_c^t \gamma^i\} - (d + e) F_{y,r}^i \quad (19)$$

We have, based on the linear tire model (Wong, 1993)

$$\dot{\lambda} = \gamma^t - \gamma^i \quad (20)$$

$$F_{y,f}^t = -C_{\alpha,f}^t \frac{v_c^t + a\gamma^t}{u_c^t} + C_{\alpha,f}^t \delta \quad (21)$$

$$F_{y,r}^t = -C_{\alpha,r}^t \frac{v_c^t - b\gamma^t}{u_c^t} \quad (22)$$

$$F_{y,r}^i = -C_{\alpha,r}^i \frac{v_c^t - c\gamma^t - (d+e)\gamma^i}{u_c^t} - C_{\alpha,r}^i \lambda \quad (23)$$

Using eqs. 17-23, the system equations in matrix form are,

$$M\dot{X} = NX + Pu \quad (24)$$

where,

$$M = \begin{bmatrix} (m^t + m^i) & -m^i c & -m^i d & 0 & 0 & 0 \\ -m^i c & (I_z^t + m^i c^2) & m^i c d & 0 & 0 & 0 \\ -m^i d & m^i c d & (I_z^i + m^i d^2) & 0 & 0 & 0 \\ 0 & 0 & 0 & 1 & 0 & 0 \\ 0 & 0 & 0 & 0 & 1 & 0 \\ 0 & 0 & 0 & 0 & 0 & 1 \end{bmatrix}$$

$$N = \begin{bmatrix} -\frac{1}{u_c^t}(C_{\alpha,f}^t + C_{\alpha,r}^t + C_{\alpha,r}^i) & -\frac{1}{u_c^t}(aC_{\alpha,f}^t - bC_{\alpha,r}^t - cC_{\alpha,r}^i + (m^t + m^i)u_c^{t2}) & \frac{(d+e)C_{\alpha,r}^i}{u_c^t} & 0 & -C_{\alpha,r}^i & C_{\alpha,r}^i \\ -\frac{1}{u_c^t}(aC_{\alpha,f}^t - bC_{\alpha,r}^t - cC_{\alpha,r}^i) & -\frac{1}{u_c^t}(a^2C_{\alpha,f}^t + b^2C_{\alpha,r}^t + c^2C_{\alpha,r}^i - m^i c u_c^{t2}) & -\frac{c(d+e)C_{\alpha,r}^i}{u_c^t} & 0 & cC_{\alpha,r}^i & -cC_{\alpha,r}^i \\ \frac{(d+e)C_{\alpha,r}^i}{u_c^t} & \left( m^i d u_c^t - \frac{c(d+e)C_{\alpha,r}^i}{u_c^t} \right) & -\frac{(d+e)^2 C_{\alpha,r}^i}{u_c^t} & 0 & (d+e)C_{\alpha,r}^i & -(d+e)C_{\alpha,r}^i \\ 1 & 0 & 0 & 0 & u_c^t & 0 \\ 0 & 1 & 0 & 0 & 0 & 0 \\ 0 & 0 & 1 & 0 & 0 & 0 \end{bmatrix}$$

$$P = \begin{bmatrix} C_{\alpha,f}^t \\ aC_{\alpha,f}^t \\ 0 \\ 0 \\ 0 \\ 0 \end{bmatrix}, \quad \dot{X} = \begin{bmatrix} \dot{v}_c^t \\ \dot{\gamma}^t \\ \dot{\gamma}^i \\ \dot{y}_c^t \\ \dot{\phi}^t \\ \dot{\phi}^i \end{bmatrix}, \quad X = \begin{bmatrix} v_c^t \\ \gamma^t \\ \gamma^i \\ y_c^t \\ \phi^t \\ \phi^i \end{bmatrix}, \quad u = [\delta]$$

In state space representation,

$$\dot{X} = AX + Bu \quad (25) \quad Y = CX + Du \quad (26)$$

where,  $A = M^{-1}N$ ,  $B = M^{-1}P$ ,  $C = \text{diag}[1 \ 1 \ 1 \ 1 \ 1 \ 1]$ ,  $D = [0]$

### 3. Steering Dynamics and Relaxation Length

A steering unit can not reach the commanded steering wheel angle instantaneously. This steering delay has to be modeled to make the simulation response of the agricultural

equipment realistic. The steering valve dynamics can be represented by (Bevly et al., 2002; Stombaugh, 1999),

$$\ddot{\delta} = \frac{d^v}{I^v} \dot{\delta} + \frac{K^v}{I^v} u_c(t) \quad (27)$$

where  $d^v$  is the damping constant,  $K^v$  is the input gain and  $I^v$  is the inertial constant, all of the steering system.

Another important dynamic mode of an agricultural vehicle steering system is the tire relaxation length. Tire relaxation length effects of an agricultural tractor can be modeled by a first order dynamic model (Bevly et. al., 2002). The relaxation length is defined as the distance a tire rolls before the steady state side slip angle is reached. A first order delay model of the slip angle due to the tire relaxation length is given by (Bevly et. al., 2002),

$$\dot{\alpha} = \frac{u}{\sigma} (\alpha_0 - \alpha) \quad (28)$$

where  $\sigma$  is relaxation length and  $\alpha_0$  is the steady state side slip angle of the tire.

Including the steering unit dynamics and the tire relaxation length dynamics, a higher fidelity tractor-and-implement model was developed and represented by eqs. 29 to 36. In the text that follows, this model will be called the 'higher fidelity model' whereas the model developed in the previous section without steering dynamics and tire relaxation length will be called the 'dynamic model'. The model equation are:

$$(m^t + m^i) \ddot{y}_c^t - m^i c \dot{\gamma}^t - m^i d \dot{\gamma}^i = -(m^i + m^t) u_c^t \gamma^t - C_{\alpha,f}^t \alpha_f^t - C_{\alpha,r}^t \alpha_r^t - C_{\alpha,r}^i \alpha_r^i \quad (29)$$

$$(I_z^t + m^i c^2) \ddot{\gamma}^t - m^i c \dot{v}_c^t + m^i c d \dot{\gamma}^i = m^i c u_c^t \gamma^t - a C_{\alpha,f}^t \alpha_f^t + b C_{\alpha,r}^t \alpha_r^t + c C_{\alpha,r}^i \alpha_r^i \quad (30)$$

$$(I_z^i + m^i d^2) \ddot{\gamma}^i - m^i d \dot{v}_c^t + m^i c d \dot{\gamma}^t = m^i d u_c^t \gamma^t + (d + e) C_{\alpha,r}^i \alpha_r^i \quad (31)$$

$$\dot{\alpha}_f^t = \frac{v_c^t}{\sigma} + \frac{a \gamma^t}{\sigma} - \frac{u_c^t}{\sigma} \delta - \frac{u_c^t}{\sigma} \alpha_f^t \quad (32)$$

$$\dot{\alpha}_r^t = \frac{v_c^t}{\sigma} - \frac{b \gamma^t}{\sigma} - \frac{u_c^t}{\sigma} \alpha_r^t \quad (33)$$

$$\dot{\alpha}_r^i = \frac{v_c^t}{\sigma} - \frac{c \gamma^t}{\sigma} - \frac{(d + e) \gamma^i}{\sigma} + \frac{u_c^t}{\sigma} \phi^t - \frac{u_c^t}{\sigma} \phi^i - \frac{u_c^t}{\sigma} \alpha_r^i \quad (34)$$

$$\dot{\tau} = -\frac{d^v}{I^v} \tau + \frac{K^v}{I^v} u_c(t) \quad (35)$$

$$\dot{\delta} = \tau \quad (36)$$

## 4. Open Loop System Analysis

John Deere (JD) 8320 agricultural tractor and typical grain cart parameters were used to simulate the models (Table 1). The tractor parameters and the formula for the z-moment of inertia were adapted from Bosserd (2007). The grain cart geometric parameters were measured using a three dimensional geometric model, and the mass was estimated to be a full load of corn. MATLAB and SIMULINK (The Mathworks, Natick, MA) were used to model and simulate the system.

Table 1: Geometric and tire parameters of a JD 8320 tractor and a typical grain cart

Tractor		Implement	
Parameters	Values	Parameters	Values
a	1.745 m	d	3.5 m
b	1.225 m	e	2.0 m

$c$	2.125 m		
$L^t$	2.97 m	$L^i$	5.5 m
$m^t$	12660 kg	$m^i$	8000 kg
$I_z^t$	67555 kg-m <sup>2</sup>	$I_z^i$	60500 kg-m <sup>2</sup>
$C_{gr}^t$	373432 N/rad		
$C_{gr}^i$	633422 N/rad	$C_{gr}^i$	373432 N/rad

For a CASE 7220 farm tractor, Stombaugh et al. (1999) calculated the ratios  $d^v/I^v = 11.4$  and  $K^v/I^v = 13.8$ . Bosserd (2007) used a time constant of 0.1 s in the steering dynamics model of the JD 8320 tractor. In this work, the parameters used were  $K^v = 10.0$ ,  $I^v = 1$  and  $d^v = 10.0$ , which corresponded to the time constant used in Bosserd (2007). A tire relaxation length  $\sigma$  of 1.5 times the tire radius was used in this work (Bevly et al., 2002). The tire radius was 1.0 m. The kinematic model developed by Karkee et al. (2007) was used to compare the open loop system responses of kinematic, dynamic and higher fidelity model.

Eigenvalue maps (Fig. 2) were used to compare the open loop characteristics of the kinematic model and the dynamic model over a range of forward velocities. The kinematic model was a third order model with two eigenvalues at the origin. The two pure integrators were representing the dynamics that the steering angle was integrated twice to get the lateral position. At a velocity of 4.5 m/s, the non-zero eigenvalue of the kinematic model was located at -0.81 whereas the dominant non-zero eigenvalue of the dynamic model was located at -0.88 (Fig. 2 b). The remaining three dynamic model eigenvalues were located at -5.33 or further to the left on the real axis. At this and lower velocities, the response of the dynamic model was not much different than that of the kinematic model as the locations of the dominant eigenvalues were not substantially different. When the forward velocity was 0.5 m/s, the three dominant eigenvalues of the models completely overlapped at 0, 0 and -0.09 (Fig. 2 a). However, when the forward velocity was increased to 7.5 m/s, the locations of the dominant non-zero eigenvalue of the two models moved apart substantially (-1.9 for dynamic model, -1.4 for kinematic model) and the fourth eigenvalue of the dynamic model moved closer to origin (-2.6). The result indicated that the kinematic model represented the tractor-and-implement dynamics as accurately as the dynamic model did in the lower range of operating velocities. However, the dynamic model was necessary to represent the additional fidelity of the system when the field operation required higher forward velocities.

The open loop characteristics of the three models were studied for a range of operating velocities. The three eigenvalues of the kinematic model represented the tractor lateral position, the tractor heading and the implement heading states. This model did not incorporate inertial dynamics of the system. As the velocity increased, the non-zero eigenvalue of the model moved to the left on the real axis, thus decreasing the system settling time (Fig. 3 a). This result was expected because the implement straightens sooner as the tractor moves faster in the forward direction.

The dynamic model represented the velocity states of the tractor-and-implement system in addition to the positional states represented by the kinematic model. At lower velocities, the three dominating eigenvalues of the dynamic model represented the tractor lateral position, the tractor heading and the implement heading states. Eigenvalues representing the velocity states (the tractor lateral velocity and the tractor and the implement yaw states) were further to the left (Fig. 3 b). Following the trend of kinematic model, the first non-zero dominant pole of the dynamic model moved further to the left as the velocity increased. However, the dominant eigenvalue moved faster in this case than in the kinematic model. More interestingly, as the velocity increased, the remaining faster eigenvalues of the dynamic model moved to the right. At a velocity of 8.0 m/s, the eigenvalues started to form complex conjugate pairs causing the system to have underdamped dynamics. As mentioned earlier, this result indicated that the

additional fidelity represented by the dynamic model comes into play at higher operating velocities.

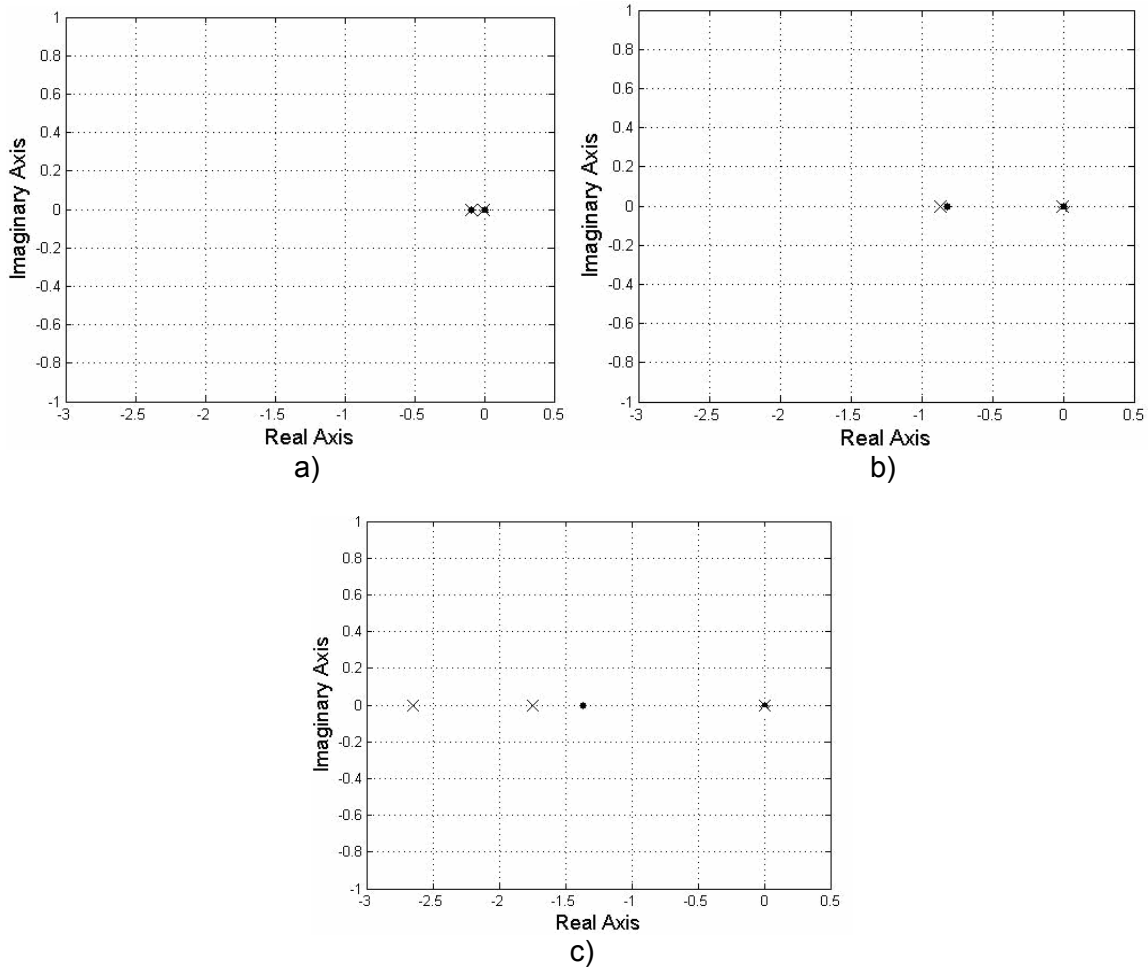
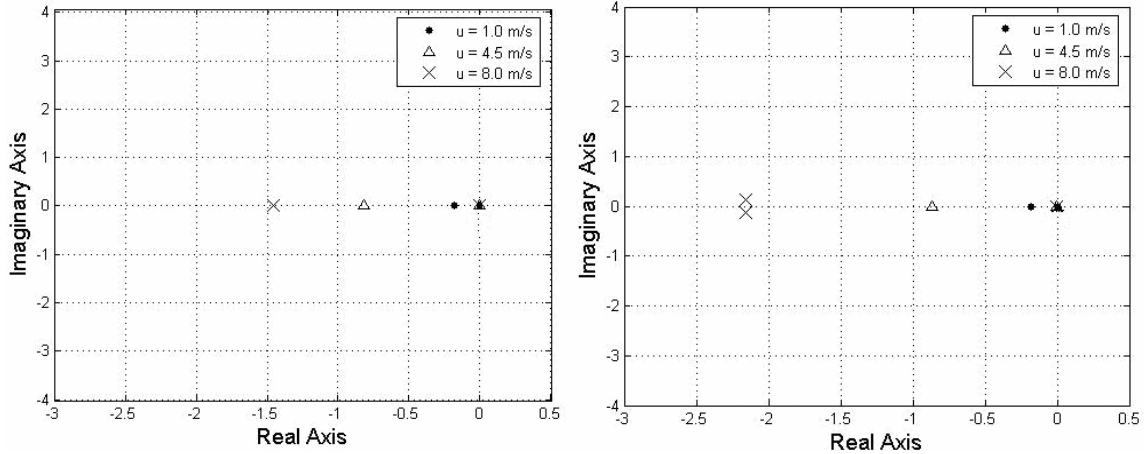


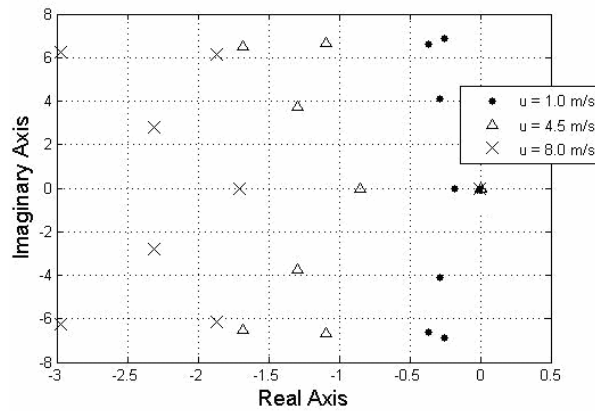
Fig. 2: Eigenvalues of the state matrix  $A$  of the tractor-and-implement system for kinematic model and dynamic model; a) 0.5 m/s (1.8 km/h), b) 4.5 m/s (16.2 km/h) and c) 7.5 m/s (27 km/h); dot – kinematic model, x – dynamic model, two eigenvalues at the origin. At 0.5 m/s, dominant eigenvalues of kinematic model and dynamic model completely overlapped. As the velocity increased, the dominant eigenvalues separated apart.

In case of the higher fidelity model, three of the eleven eigenvalues were located at origin. The third pure integrator was a part of the steering dynamics, which was used to get the steering angle from the hydraulic flow. The second eigenvalue of the steering dynamics was located at -10, which was the fastest eigenvalue among the 11 eigenvalues of the open loop system at 4.5 m/s (Fig. 3 c). Interestingly, in this case also, the positional states described in the kinematic model and the dynamic model were clearly identifiable and dominating the system. However, the tire relaxation length states coupled with the inertial states and formed complex conjugate pairs. At lower velocities, these conjugate pairs were highly underdamped and very close to the imaginary axis to cause significant oscillation and overshoot in the system response. At a very low velocity, the model might be marginally unstable, which was unlikely to happen in the real agricultural vehicle. This result indicated that the tire relaxation length dynamics with constant relaxation length parameter did not represent the reality accurately at lower velocities. As the velocity increased, the eigenvalues systematically moved further to the left while the imaginary parts of the complex conjugate pairs remained almost constant. This

result indicated that in the velocity range of 1.0 m/s to 8.0 m/s, the open loop system became faster and more damped as the operating velocity increased.



a) Kinematic model, two eigenvalues at origin      b) Dynamic model, two eigenvalues at origin



c) Higher fidelity dynamic model, three eigenvalues at the origin

Fig. 3: Eigenvalues of the state matrix A of the tractor-and-implement system for forward velocities of 1.0 m/s, 4.5 m/s and 8.0 m/s. a) Kinematic Model (Karkee et al., 2007), b) Dynamic Model and c) Higher Fidelity Dynamic Model. All eigenvalues were real and negative, which showed that the systems were stable. Several eigenvalues of the dynamic and higher fidelity model were located further to the left from the left margin.

It was important to test the controllability and the observability of the model with the parameters selected. The controllability matrix of the dynamic model has a full rank, which means that any state of the system can be driven to zero from an arbitrary initial value. Observability plays a key roll in the controller design. The system was observable with the assumption that the tractor lateral position, tractor heading angle and implement heading angle were the measured variables. This characteristic provided an opportunity to estimate three immeasurable states namely tractor lateral velocity, tractor yaw rate and implement yaw rate, which were necessary to have a full state feedback closed loop system to be discussed in the next section. The higher fidelity model was also controllable. Because the slip angle states and the steering position and rate states were not measured, partial state feedback was used to study the higher fidelity closed loop system.

## 5. Closed Loop Analysis

The closed loop characteristics of the kinematic model was studied by Karkee et al. (2007). However, the kinematic model failed to represent the higher order dynamics of the tractor-and-implement system, which was essential at higher velocities. It was important to study the closed loop characteristics of the dynamic model to extend the possibility of the tractor-and-implement guidance system in higher velocity operations.

To study the closed loop characteristics of the tractor-and-implement dynamic model, a linear quadratic regulator (LQR) was used to close the loop around the system (Fig. 4). The output signal we wanted to make as small as possible in the shortest possible time was  $y(t)$ . The command input to the system was  $p(t)$ .

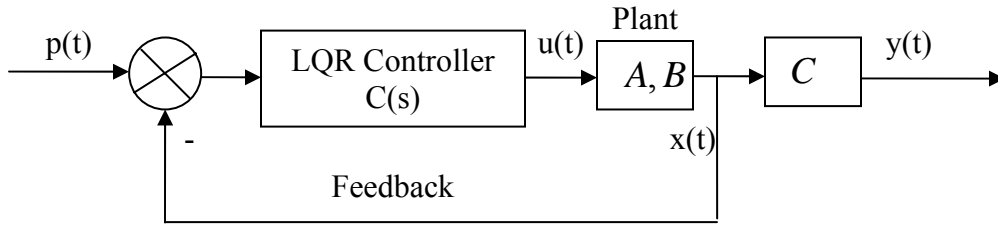


Fig. 4: Block diagram of a feedback controller. The command input to the system is  $p(t)$  and output is  $y(t)$ . The control effort is  $u(t)$ .

The controller transfer function  $C(s)$  was found in such a way that minimized the objective function (Franklin et al., 2002),

$$J = \int_0^{\infty} (x^T Q x + u^T R u) dt \quad (37)$$

The state vector of the dynamic model consisted of the lateral velocity of the tractor CG, yaw rates of the tractor and the implement, y-axis position of the tractor CG and heading angles of the tractor and the implement. The last three states were measurable using high accuracy GPS receivers. Because the system was observable, an estimator could be designed to estimate the remaining three states. Assuming all six states of the state vector  $X$  could be measured (or estimated) and fed back, the control law, with zero command input  $p(t)$  became,

$$u(t) = -Kx(t) \quad (38)$$

The closed loop system with state feedback controller was then given by,

$$\dot{x} = A_c x \quad (39)$$

$$\text{where, } A_c = (A - BK)$$

The LQR controller design process seeks to find the control law,  $K$ , so that the optimization goal (Eq. 37) is reached. Matlab 'lqr' utility was used to find  $K$  and simulate the response of the closed loop system. The 'lqr' utility solves an algebraic Riccati equation associated with the system to obtain the gain  $K$ . Two matrices  $Q$  and  $R$  were used to establish a tradeoff between the control effort and the control output. Since there were six states in the system,  $Q$  needed to be a 6x6 matrix where as  $R$  needed to be just a scalar as there was only one input, the steering angle. The first set of guesses of  $Q$  and  $R$  in the iterative procedure of the controller design did not penalize either of the controlled outputs and control effort (Eq. 40).

$$Q = \text{diag}[1 \ 1 \ 1 \ 1 \ 1 \ 1], \ R=1 \quad (40)$$

The dynamic model closed loop system with the first choice of the LQR parameters and the forward velocity of 4.5 m/s was stable and responded very quickly to the tracking errors. The dominant eigenvalue of the closed loop system was -0.87, which corresponded to a settling time of 4.6 s and settling distance of 20.7 m. The dominant damping ratio was 0.7. However, for the tractor initial off-track error of 5 m and tractor and implement initial heading errors of  $20^\circ$ , the steering angle and steering rate were larger than the practical limits of  $\pm 35^\circ$  and  $6^\circ/\text{s}$  respectively (Karkee et al., 2007; Takigawa et al., 1998). Because no steering dynamics were modeled, it was implicitly assumed that the steering wheel could be rotated by any angle instantaneously. The steering history improved when the control effort was penalized (Fig. 5). However, even with a large value of R, the instantaneous jump at  $t = 0$  s and quick ramp in the interval of  $0 < t < 1$  s still remained in the steering angle history. Due to this problem, the higher fidelity model was used in further analysis of the closed loop system.

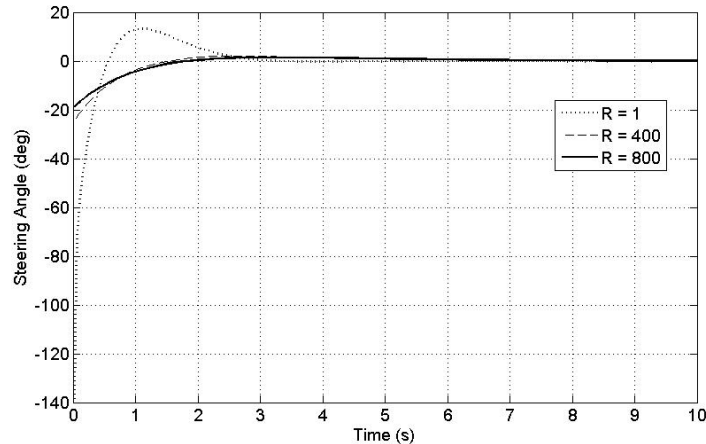


Fig. 5: Steering angle history produced by the dynamic model closed loop system at a velocity of 4.5 m/s. Tractor initial off-track error was 5 m and tractor and implement initial heading error was  $20^\circ$ . At  $t = 0$ , steering angle jumped to a large value and steering rate formed a spike. Because no steering dynamics were modeled, it was assumed that the steering wheel could be rotated instantaneously. As the control effort was penalized more, the steering history improved.

Five states (three slip angles, steering rate and steering angle states) of the eleven state higher fidelity model were not measured. So, the closed loop system with the higher fidelity model used partial state feedback. The control effort penalty R was 800. The steering angles and rates were more realistic in this case (Fig. 6). For the tractor initial off-track error of 5 m and tractor and implement initial heading error of  $20^\circ$ , the steering angle reached only up to  $11^\circ$  while keeping steering rate reasonably low. There was no instantaneous jump at  $t = 0$  s as in the dynamic model closed loop system. In the beginning, the steering rate was about  $10^\circ/\text{s}$ , which is towards the upper limit of the practical steering rate. However, this rate lasted for less than a second, which should not have substantial effect on the accuracy of the non-linear simulation results.

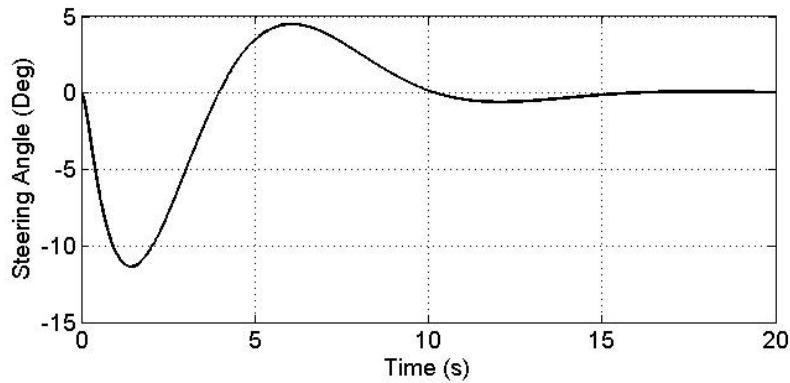


Fig. 6: Steering history generated by the higher fidelity closed loop system. The tractor initial off-track error was 5 m and tractor and implement initial heading error was  $20^\circ$ .

All eigenvalues of the closed loop system at the velocities 1.0 m/s, 4.5 m/s and 8.0 m/s were located in the left half plane, which showed the closed loop system was stable in this range of velocities (Fig. 7). At each velocity, a conjugate pair of eigenvalues dominated the response. At 1.0 m/s, all 10 eigenvalues were located close to the origin and close to the dominant pair. Most of the complex pairs were highly underdamped. Meantime, there were two real eigenvalues nearby the dominating pair, which helped to improve the system damping. As the velocity increased, the closed loop eigenvalues moved to the left as in the open loop system. However, the dominant conjugate pair diverged while moving to the left, which decreased the damping ratio. Consequently, the closed loop system became faster but more oscillatory as the velocity increased (Fig. 7 – Fig. 9).

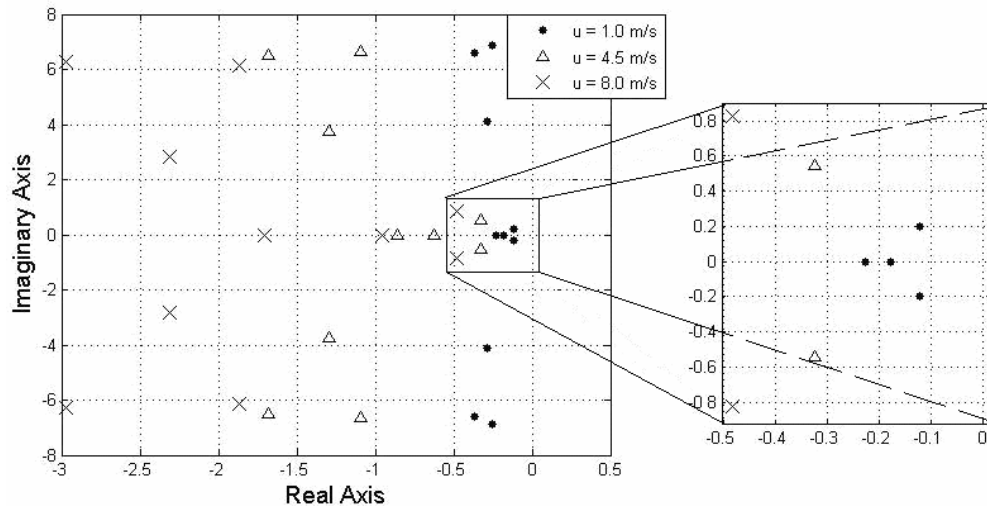


Fig. 7: Eigenvalues of the state matrix  $A_c$  of the higher fidelity model closed loop system for forward velocities of 1.0 m/s, 4.5 m/s and 8.0 m/s. Control effort penalty  $R$  was 800. All eigenvalues were located in the left half plane, which showed the closed loop system was stable in the range of velocities from 1.0 m/s to 8.0 m/s.

The closed loop characteristics of the higher fidelity model were further assessed using settling distance and damping ratio of the response over a set of control effort penalty  $R$  and a range of operating velocities. For  $R = 1$ , the settling distance of the closed loop tractor-and-implement system remained almost constant in the operating velocity range of 0.5 m/s to 7.0 m/s (Fig. 8). As the velocity increased beyond 7.0 m/s, the settling distance started to rise gently. In contrast, for  $R = 200, 400$  and  $800$ , the settling distance started at about 24 m and increased almost linearly over the velocity range from 0.5 m/s to 10 m/s. From the eigenvalue

map (Fig. 7), we observed that the settling time decreased as the velocity increased. However, the rate of decrement lagged the rate of velocity increment so that the settling distance did not remain constant. The higher the value of  $R$ , the faster the settling distance increased with the increasing velocity. This trend of settling distance was expected. When the control effort was penalized harder, the steering effort became less aggressive, which caused the system to respond slowly.

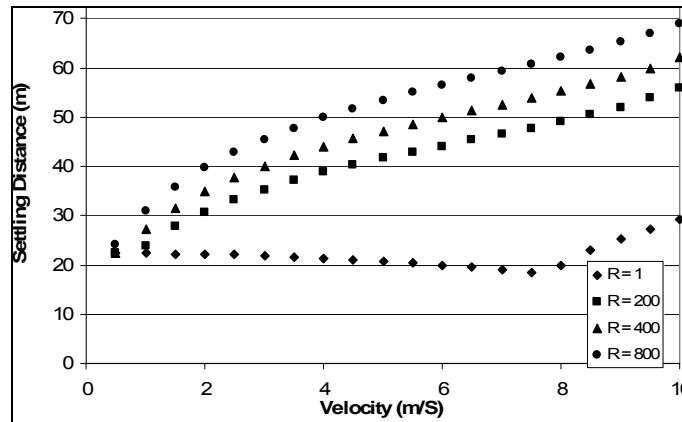


Fig. 8: Higher fidelity model closed loop settling distance over a range of forward velocities and different values of  $R$ . The settling distance remained almost constant for  $R=1$  and increased almost linearly with velocity for  $R = 200, 400$  and  $800$ .

Generally, the dominant pair damping ratio decreased as the velocity increased, which showed the closed loop system was more oscillatory at higher velocities. The result also showed that the damping ratio with smaller  $R$  decreased faster with increasing velocity. This trend of damping ratio indicated that the control effort must be penalized more as the operating velocity increases in order to maintain the same level of damping in the closed loop response. The damping ratios were quite small in the velocity range of 0.5 m/s to 10.0 m/s. However, there always were one or more real eigenvalues located nearby the dominant conjugate eigenvalue pair. In many cases, the real eigenvalue(s) were even dominating over the complex conjugate pairs. These real eigenvalues forced the system response decay faster than suggested by the conjugate eigenvalue pair. For  $R = 800$  and forward velocity of 4.5 m/s, the dominant pair damping ratio was 0.51, which corresponded to the closed loop maximum overshoot of 15%. As discussed in the next section, simulated value of the closed loop maximum overshoot was substantially less than the maximum overshoot of 15% calculated from the dominant eigenvalue pair.

For  $R = 800$ , the dominant eigenvalue characteristics of the higher fidelity model closed loop system remained reasonable over a wide range of operating velocities. The performance in terms of stability, settling time and damping ratio remained well within the off-road vehicle guidance system design specification (Karkee et al., 2007) in the practical operating velocity range of 0.5 to 7.0 m/s (Stombough et al., 1999).

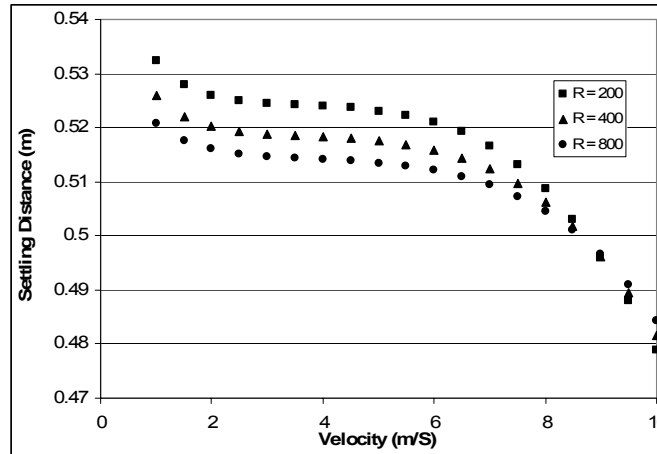


Fig. 9: Dominant damping ratio of the higher fidelity model closed loop system response over a range of forward velocities and different values of R. For R = 200, 400 and 800, the damping ratio remained almost constant in the velocity range of 2.0 m/s to 6.0 m/s. The damping ratio started to decrease rapidly as the velocity was increased beyond 7.0 m/s.

## 6. Simulation Results and Discussion

To study the closed loop response of the tractor-and-implement model, an LQR controller was used in the feedback loop of the higher fidelity dynamic model. The closed loop system response was evaluated using the simulation plots.

The closed loop system brought the initial off-track and heading errors of the tractor-and-implement system back to zero (Fig. 10). The settling time for the tractor off-track and heading error was about 12 s to 13 s for a forward velocity of 4.5 m/s. Similarly, the implement off-track and heading error settling time was about 14 s to 15 s. These settling times were slightly higher than the settling time calculated from the dominant eigenvalues. The discrepancy was because of the effect of other real eigenvalue(s), which were located nearby the dominant conjugate eigenvalue pair. From the simulation, it was observed that the tractor-and-implement system kept going in the initial direction for some period of time (Fig 10). This sluggish initial response was expected because the relaxation length dynamics introduced delays to the steering response of the vehicle model.

The closed loop system was substantially underdamped. The dominant eigenvalue of the closed loop system showed that the response would have 15% maximum overshoot. However, the simulated off-track error showed only about 10% overshoot (Fig. 10). The overshoot was subsided due to the damping effect of other two real eigenvalues of the closed loop system, which were close enough to affect the response of the dominant conjugate eigenvalue pair.

The heading errors of the response went up to 24° and 20° respectively for the tractor and the implement for an initial heading error of 20° and tractor off-track error of 5m. Similarly, the steering angle reached up to 11°. The small angle assumption used in the linearization of the model may not hold beyond 10°. These angles remained above 10° for some time (<5 s) in the transient period, which will have no effect in the steady state performance but may have some effect in the transient response. The maximum value of the heading and steering angles remained below 10° when the tractor initial off-track error was reduced to 3 m and the tractor and implement initial heading error was reduced to 10°.

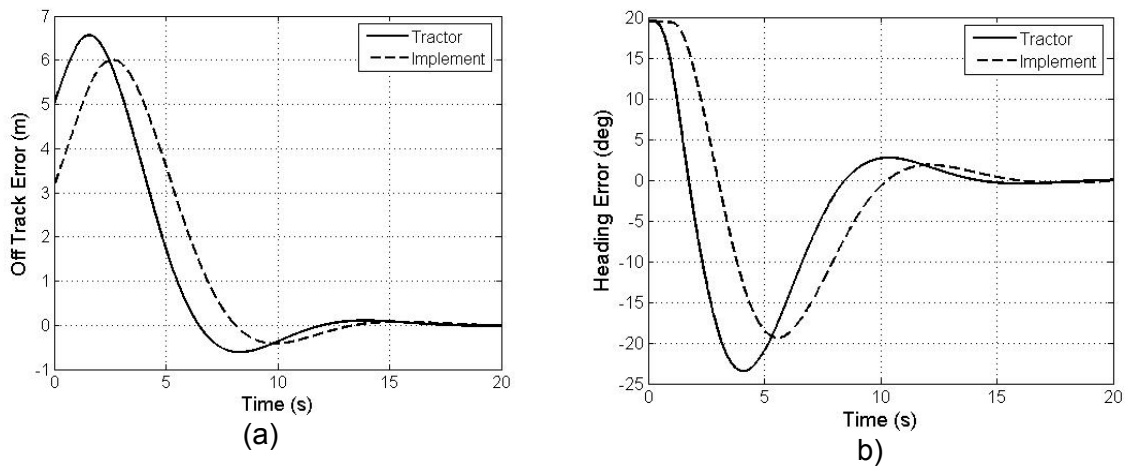


Fig. 10: Simulation response of the closed loop system; a) tractor and implement off-track error b) tractor and implement heading error. The forward velocity was 4.5 m/s. The initial tractor off-track error was 5 m and initial tractor and implement heading error was 20°.

The closed loop system was stable for a wide range of operating velocities. The system response was within the nominal performance specification of an off-road vehicle guidance system (Karkee et al., 2007). Because the open loop system had three eigenvalues at the origin, the steady state error was driven to zero without having an integrator in the feedback loop. These simulation studies provided understanding of the closed loop characteristics of the tractor and towed implement system, which opened up new opportunity to develop tractor and towed implement guidance controllers using the feedback from the tractor mounted position and heading sensors and the implement mounted heading sensor simultaneously.

## 7. Conclusion

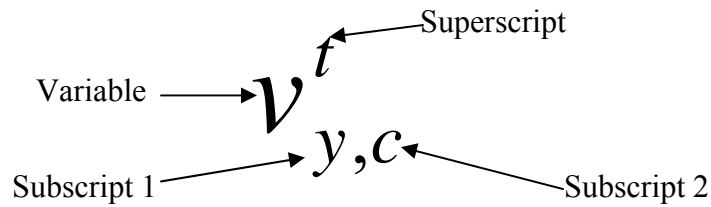
A dynamic tractor and implement model was developed using the interaction at the hitch point. The steering dynamics and the tire relaxation length dynamics were also incorporated. Open loop and closed loop system characteristics of the model were studied. A LQR guidance controller was used to close the loop around the system. From this work, we can conclude that:

- In the lower range of operating velocities, the kinematic tractor and towed implement model represents the system dynamics as accurately as the dynamic model does. The dynamic model is necessary to represent higher order dynamics of the system, which is essential when the field operation requires higher forward velocities.
- A stable tractor and implement guidance controller for high speed operation can be developed using the feedback from the tractor mounted position and heading sensors and the implement mounted heading sensor.

### Acknowledgements:

This research was supported by Hatch Act and State of Iowa funds. (Journal paper of the Iowa Agriculture and Home Economics Experiment Station, Ames, Iowa, Project No. 3612.)

## Notation and List of Variables:



- Variable:** The variable itself.  
Big or bold letter – vector or matrix, small letter – scalar
- Superscript:** Denotes whether the variable is related to tractor or implement  
t – tractor, i – implement
- Subscript 1:** Specifies the co-ordinate axis the variable corresponds to.  
x – x axis, y – y axis, z – z axis
- Subscript 2:** Specifies the location the variable corresponds to.  
f – front tire axle, r – rear tire axle, c – center of gravity, p – toe pin (hitch point)

### List of variables

- a distance between front axle and CG of tractor
- b distance between rear axle and CG of tractor
- c distance between hitch point and CG of tractor
- d distance between hitch point and CG of implement
- e distance between rear axle and CG of implement
- L wheelbase
- F force
- u longitudinal velocity
- v lateral velocity
- r yaw rate
- y position of CG in y- axis of the world co-ordinate system
- $\psi$  heading angle
- $\delta$  steering angle
- $\alpha$  side slip angle or the angle between the direction the tire is going and the direction it is facing. The velocity vector to the right of the tire is positive and reverse is negative.
- $\lambda$  angle between tractor heading and implement heading
- $\alpha_0$  steady state side slip angle
- $\sigma$  relaxation length
- $l^v, d^v$  and  $K^v$  steering unit actuator parameters
- $u_c(t)$  steering unit actuator input
- m mass
- $I_z$  yaw moment of inertia
- $C_\alpha$  cornering stiffness
- n size of state (square) matrix A
- $X_c$  control state vector
- Q LQR controlled output penalty matrix
- R LQR control effort penalty matrix

## References:

- Bell, T. 1997. Precision Robotic Control of Agricultural Vehicles on Realistic Farm Trajectory. *PhD dissertation*, Stanford University.
- Bell, T. 2000. Automatic Tractor Guidance using Carrier-phase Differential GPS. *Computers and Electronics in Agriculture* 25(2000):53-66.
- Benson, E., T. Stombaugh, N. Noguchi, Will J., and J.F. Reid. 1998. An Evaluation of a Geomagnetic Direction Sensor for Vehicle Guidance in Precision Agriculture Applications. *ASAE Paper # 983203*. ASAE, St. Joseph, MI.
- Benson, E. R., J. F. Reid, and Q. Zhang. 2001. Machine Vision based Steering System for Agricultural Combines. *ASAE Paper # 01-1159*. ASAE, St. Joseph, MI.
- Bevly, D. M. 2001. High Speed, Dead Reckoning, and Towed Implement Control for Automatically Steered Farm Tractors using GPS. *PhD dissertation*, Stanford University.
- Bevly, D. M., J. C. Gerdes, and B. W. Parkinson. 2002. A New Yaw Dynamic Model for Improved High Speed Control of a Farm Tractor. *Journal of Dynamic Systems, Measurement, and Control* 124: 659-667.
- Bosserd II, J. A. 2007. Investigation of roll angle feed-forward control and look-ahead functions to improve automatic guidance on sloped terrain. *Master's Thesis*, Iowa State University.
- Bryson, A. E., and Y. C. Ho. 1975. *Applied Optimal Estimation*. Hemisphere Publishing Corp.
- Choi, C. H., D. C. Erbach, and R. J. Smith. 1990. Navigational Tractor Guidance System. *Transactions of the ASAE* 33(3): 699-706.
- Feng, L., Y. He, Y. Bao, and H. Fang. 2005. Development of Trajectory Model for a Tractor-Implement System for Automated Navigation Applications. *Instrumentation and Measurement Technology Conference Ottawa, Canada, May 17-19, 2005*.
- Franklin, G. F., J. D. Powell, and A. Emami-Naeini. 2002. *Feedback Control of Dynamic Systems*. Upper Saddle River, NJ, Prentice Hall.
- Gerrish, J.B., and T.C. Surbrook. 1984. Mobile robots in agriculture. *In Proc. of First International Conference on Robotics and Intelligent Machines in Agriculture*. ASAE, St. Joseph, MI. 30-41.
- Gerrish, J.B., B.W. Fehr, G. R. Van Ee, and D. P. Welch. 1997. Self-steering tractor guided by computer-vision. *Applied Engineering in Agriculture* 13(5): 559-563.
- Graham, D. and D. McRuer. 1961. *Analysis of Nonlinear Control Systems*. John Wiley & Sons.
- Greenwood, D. T. 1965. *Principles of Dynamics*. Englewood Cliffs, NJ, Prentice Hall.
- Julian, A.P. 1971. Design and performance of a steering control system for agricultural tractors. *J. Agric. Eng. Res.* 16(3): 324-336.
- Karkee, M., B. L. Steward, and S. A. Aziz. 2007. Distributed Virtual Reality Assisted Steering Controller Design for Off-road Vehicle and Implement Tracking. *ASABE Paper No. 073006*. ASAE, St. Joseph, MI.
- Lumkes, J. H. 2002. *Control Strategies for Dynamic Systems*. New York, N.Y., USA: Marcel Dekker, Inc.
- Noguchi, N., J. F. Reid, E. Benson, J. Will., and T. Stombaugh. 1998. Vehicle Automation System Based on Multi-sensor Integration. *ASAE Paper # 983111*. ASAE, St. Joseph, MI.
- Noh, K. M. and D.C. Erbach. 1993. Self-tuning Controller for Farm Tractor Guidance. *Transactions of the ASAE* 36(6): 1583-1594.
- O'Connor, M., T. Bell, G. Elkaim, and B. Parkinson. 1996. Automatic Steering of Farm Vehicles using GPS. *Third international conference on precision agriculture*. Minneapolis, MN, June 23-26, 1996.

- O'Connor, M. L. 1997. Carrier-Phase Differential GPS for Automatic Control of Land Vehicles. *PhD thesis*, Stanford University.
- Ogata, K. 1978. *System Dynamics*. Prentice Hall.
- Oksanen, T. and A. Visala. 2004. Optimal Control of Tractor-trailer System in Headlands. *Automation Technology for Off-Road Equipment Conference*. Kyoto, Japan, 7-8 Oct, 2004.
- Ollis, M., and A. Stentz. 1996. First Results in Vision-based Crop Line Tracking. *Proceedings of the IEEE Robotics and Automation Conference*. Minneapolis, MN, 951–956.
- Palm, W. J. 2005. *System Dynamics*. New York, N.Y., USA: The McGraw-Hill Companies, Inc.
- Reid, J. F., Q. Zhang, N. Noguchi, and M. Dickson. 2000. Agricultural Automatic Guidance Research in North America. *Computers and Electronics in Agriculture* 25(2000): 155-167.
- Smith, L.A., R.L. Scharfer, and R. E. Young. 1985. Control Algorithms for Tractor-implement Guidance. *Transactions of the ASAE* 28(2): 415-419.
- Stombaugh, T. S., E. R. Benson, and J. W. Hummel. 1998. Automatic Guidance of Agricultural Vehicles at High Field Speeds. *ASAE Paper No. 983110*. ASAE, St. Joseph, MI.
- Stombaugh, T. S., E. R. Benson, and J. W. Hummel. 1999. Guidance Control of Agricultural Vehicles at High Field Speeds. *Transactions of ASAE* 42(2): 537-544.
- Van Zuydam, R. P. 1998. Centimeter-Precision Guidance of Agricultural Implements in the Open Field by Means of real Time Kinematic (RTK) GPS. *Fourth International Conference on Precision Agriculture*. Saint Paul, MN, 19-22 July, 1998.
- Wong, J.Y. 1993. *Theory of Ground Vehicles*. New York, N.Y., USA: John Wiley & Sons Ltd.